

CrystEngComm

Accepted Manuscript



This is an *Accepted Manuscript*, which has been through the Royal Society of Chemistry peer review process and has been accepted for publication.

Accepted Manuscripts are published online shortly after acceptance, before technical editing, formatting and proof reading. Using this free service, authors can make their results available to the community, in citable form, before we publish the edited article. We will replace this *Accepted Manuscript* with the edited and formatted *Advance Article* as soon as it is available.

You can find more information about *Accepted Manuscripts* in the [Information for Authors](#).

Please note that technical editing may introduce minor changes to the text and/or graphics, which may alter content. The journal's standard [Terms & Conditions](#) and the [Ethical guidelines](#) still apply. In no event shall the Royal Society of Chemistry be held responsible for any errors or omissions in this *Accepted Manuscript* or any consequences arising from the use of any information it contains.

Structural Trends in Hybrid Perovskites, $[\text{Me}_2\text{NH}_2] \text{M} [\text{HCOO}]_3$ (M=Mn, Fe, Co, Ni, Zn).
Computational Assessment Based on Bader Charge Analysis.

Monica Kosa* and Dan Thomas Major

*Department of Chemistry, Faculty of Exact Sciences and the Lise Meitner-Minerva Center of
Computational Quantum Chemistry, Bar-Ilan University, Ramat-Gan 52900, Israel*

Abstract (~50 words according to communication template)

Topological analysis of the electron density of hybrid perovskites with different transition metal atoms indicate that the variation of the cell size depends on the extent of charge transfer from metal to oxygen rather than on the identity of the transition metal atom alone. The metal-oxygen interaction is less polarized and thus greater covalent vs. ionic contribution is expected along the first row transition metal series.

Keywords: MOF, perovskite, Bader charge analysis, DFT.

**Corresponding Author: monica.kosa.shtaif@gmail.com*

Introduction

Hybrid framework materials have attracted enormous attention in past decades both due to the variety of possible structures and the emerging technological applications. In particular, porous frameworks received enormous attention due to their applications arising from the solvent free - guest accessible volume.¹ The variation of the metal and the multifunctional organic ligands led to unprecedented performance in the fields of gas storage and separation, biomedical applications, ion conduction, chemical and photo catalysis,² as well as crystal-free crystallization.³

Hybrid framework materials without guest accessible pores have been investigated much less. Their potential applications are related to luminescent, electric and magnetic traits.^{4, 5 6} For both porous and non-porous hybrid framework materials, the structure, stability and mechanical response are crucial descriptors which control their incorporation in devices at industrial scales.⁷

In the past decade, series of metal organic frameworks comprised of transition metal atoms interconnected by formate (HCOO) ligands, with the perovskite topology, i.e. ABX_3 , $[Me_2NH] M [HCOO]_3$ ($M=Mn, Fe, Co, Ni, Zn$) were investigated both experimentally⁸⁻¹¹ and computationally¹²⁻¹⁴ due to their multiferroic behavior. In these multiferroic frameworks the electrical order involves hydrogen bonding. Interestingly, a recent experimental investigation of their mechanical properties revealed that the elastic mechanical response depend on the nature of the metal ions.¹⁵ The measured Young moduli of Mn and Zn are very similar, ~19 GPa, while those of Co and Ni are higher, 21.7 and 24.3 GPa. This study demonstrates that the mechanical properties of hybrid framework materials are coupled to the electronic structure of transition metal atoms. Namely, the Young modulus could be correlated to the ligand field stabilization energy in $[Me_2NH_2] M [HCOO]_3$ for $M = Mn, Co Ni$ and Zn. It has previously been demonstrated that the applied mechanical pressure in MOFs, is accommodated by the relatively flexible metal-oxygen cores (while the organic ligands remain almost intact in the elastic limit).^{16, 17} That implies that transition metal-formate interactions in $[Me_2NH_2] M [HCOO]_3$ are crucial for the observed mechanical response. To further understand the structure-property relationship in hybrid frameworks with perovskite topology, and the dependence of mechanical properties on their electronic structure,¹⁵ we investigate the charge density of $[Me_2NH_2] M [HCOO]_3$ ($M=Mn, Fe, Co, Ni, Zn$) based on density functional theory (DFT). Specifically, we perform a topological investigation of the electron density employing Bader charge analysis. The charge distribution in these systems is particularly important due their ferroelectric traits.

Computational methods

The rhombohedral simulation cell, containing two formula units of $[\text{Me}_2\text{NH}_2] \text{M} [\text{HCOO}]_3$ was used, assuming antiferromagnetic ordering of the metal atoms. The visual representation of the simulation cell can be found in the Electronic Supporting Information, ESI, SF1.

DFT calculations were performed with the VASP 5.2.12 program,¹⁸⁻²¹ using projector augmented wave (PAW)^{22,23} pseudo potentials (PP), a 550 eV plane wave energy cutoff, Γ -centered k-point mesh, spacing of at least 0.3 \AA^{-1} in conjunction with the PBE²⁴ functional. The PBE functional was augmented with a Hubbard on-site potential, $U=2, 4, 6 \text{ eV}$, within the general GGA+U approach²⁵ and the local dispersion correction, termed DFT+D3.²⁶ All compounds were computed with the aforementioned U values (complete set of data is available in the, ESI, ST1). Bader charge analysis²⁷ was performed on the all-electron densities charge files (the core density was generated from the PP files).²⁸⁻³⁰ Correct valence electron count, based on the Bader partitioning, was achieved using the default grids, specified in ESI, ST2. The variation of both cell parameters and the Bader charges and volumes (see ESI, ST3) is minor with respect to the U value. The discussion in the text is based on $U=2$. The variation of the electronic density of states, as function of U may vary substantially for certain transition metal perovskites, see ESI, SF2. The visualization of the isodensity surfaces was done with the VESTA program.³¹

Results and Discussion

Figure 1 shows the calculated system volume as well as the total volume decomposed into each component of the $[\text{Me}_2\text{NH}_2] \text{M} [\text{HCOO}]_3$ system, as computed by the Bader charge analysis method.

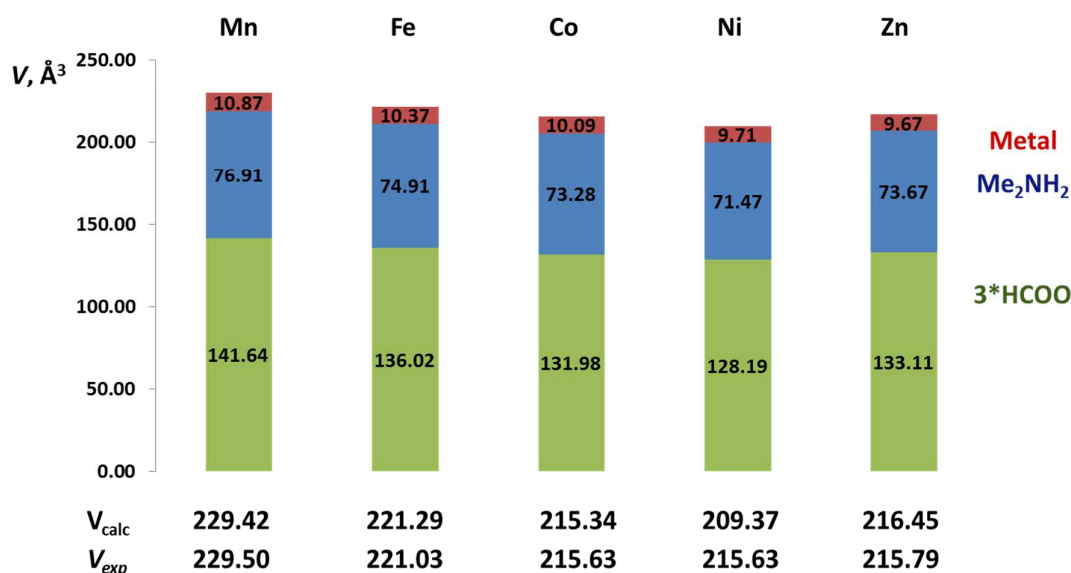


Figure 1. Calculated (V_{calc}) and experimental (V_{exp})^{8, 10, 11} volumes, normalized per 1 formula unit of $[\text{Me}_2\text{NH}_2] \text{M} [\text{HCOO}]_3$, $\text{M} = \text{Mn, Fe, Co, Ni, Zn}$.

There is good agreement between the calculated and experimental total volumes, V_{calc} and V_{exp} , for $\text{M} = \text{Mn, Fe, Co, Zn}$. For $\text{M} = \text{Ni}$ there is a slight deviation. The decomposition of the total volume, to its constituent chemical building units, i.e. M , Me_2NH_2 and three HCOO ligands, reveals that the organic formate (HCOO) ligands occupy the majority of the space in each system, designated in green in Figure 1. However, the volume of the formate ligands is different in each of the systems, i.e. $\text{M} = \text{Mn, Fe, Co, Ni, Zn}$. For example, for $\text{M} = \text{Mn}$, the formate ligands occupy the largest absolute volume, 141.64 \AA^3 while for $\text{M} = \text{Co}$, the formate ligands occupy a lower absolute volume of 131.98 \AA^3 . The variation in the formate ligands volume spans a range of $\sim 13.45 \text{ \AA}^3$. In the Bader charge and volume analysis, the boundaries of each atom, which control the particular atomic volume, are determined according to the minimum electron density path. This implies that different volumes of the formate ligands for the $\text{M} = \text{Mn, Fe, Co, Ni, Zn}$ based perovskites results from the different electron density encompassed within those volumes. This will be discussed later in the manuscript.

Similarly to formate ligands, the volume of the dimethylammonium (Me_2NH_2) moiety changes as function of the metal and has a maximum value of 76.91 \AA^3 for $\text{M} = \text{Mn}$. However, in contrast to the formate ligands, the variation of the volumes of dimethylammonium is small, spanning a range of 5.44 \AA^3 . According to the Bader

partitioning scheme, the volume occupied by the dimethylammonium ion represents the volume of the cavity formed by the anionic (metal-formate) framework.

The volume of the metal atoms varies between 10.87 for Mn and 9.67 Å³ for Zn, spanning a range of only ~1.2 Å³. These computed volumes are consistent with the decreasing ionic and crystal radii along the first row 3d transition metals.^{32,33}

The partitioning of the total volume to its chemical building blocks show that the change of the cell parameters and the unit cell volumes can be attributed mainly to the changes in the volumes of the formate ligands and not to the change in the effective size of transition metal ions.

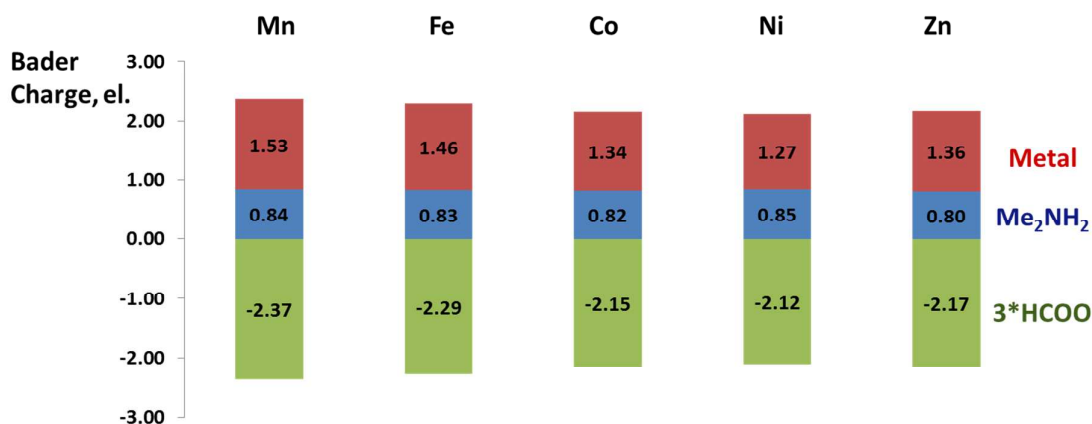


Figure 2. Bader charges of [Me₂NH₂]₃M [HCOO]₃, M = Mn, Fe, Co, Ni, Zn.

The Bader charge partitioning scheme, shown in figure 2, reveals that in hybrid perovskites the charges of the metal atoms (designated in red in figure 2) and the formate ligands (designated in green in figure 2) vary considerably, while only minor changes are observed for the dimethylammonium moiety (designated in blue). The absolute charges of the dimethylammonium vary between the maximal value of +0.85 a.u. for M=Ni to the minimal value of +0.80 a.u. for M=Zn. That is, the total integrated electron density within the cavity of dimethylammonium practically does not change upon the variation of the metal. This is consistent with the fact that the dimethylammonium ligand cannot accept or donate large amount of charge.

The charges of the metal atoms vary between the +1.54 for M=Mn and +1.28 a.u. for M=Ni. The reduction of positive charge, i.e. gain of the negative electron charge, is consistent with increasing Pauling electronegativity for Fe, Co and Ni, forming a linear correlation, while for Mn and Zn, with 3d⁵ and 3d¹⁰ configurations, there is a deviation from the linear trend (see ESI, SF3 for details).

The decrease in the positive charge of the metal atoms is concomitant to the decrease in the negative charge of the formate ligands. The greatest negative charge of the formate ligands of -2.37 a.u. is found in $[\text{Me}_2\text{NH}_2] \text{Mn} [\text{HCOO}]_3$, while the lowest negative charge of the formate ligands of -2.12 a.u. is found in $[\text{Me}_2\text{NH}_2] \text{Ni} [\text{HCOO}]_3$.

The significant variation of the charges of the metal atoms and the formate ligands in $[\text{Me}_2\text{NH}_2] \text{M} [\text{HCOO}]_3$, $\text{M} = \text{Mn, Fe, Co, Ni, Zn}$, i.e. the polarization of the metal oxygen bond, imply that for this series of transition metal atoms, the bonding, i.e. the degree of ionic and covalent contributions in the metal oxygen interaction, may vary as well. That is, in $[\text{Me}_2\text{NH}_2] \text{Mn} [\text{HCOO}]_3$ the Mn-oxygen interaction is the most polarized (based on the Bader charge distribution in figure 2), leading to an increase in ionic vs. covalent contribution in the bond. In $[\text{Me}_2\text{NH}_2] \text{Ni} [\text{HCOO}]_3$, the nickel oxygen interaction is the least polarized and thus an increase in covalent vs. ionic contribution is expected. The changes in ionic and covalent contributions in the metal-oxygen bonds are manifested in the variations in the spatial distribution of the electron density. For the more ionic systems the electron cloud is to a greater extent localized on the atoms, while in the more covalent systems the electron density is shifted towards the interatomic region. This scenario is observed for the entire $[\text{Me}_2\text{NH}_2] \text{M} [\text{HCOO}]_3$ series investigated herein.

Figure 3 shows the computed charge density for the two extreme cases: $[\text{Me}_2\text{NH}_2] \text{Mn} [\text{HCOO}]_3$ and $[\text{Me}_2\text{NH}_2] \text{Ni} [\text{HCOO}]_3$. The encircled interatomic region clearly shows enhanced electron density for $\text{M}=\text{Ni}$ compared to $\text{M}=\text{Mn}$. The M-O bond distance varies from 2.182 to 2.258 Å for $\text{M}=\text{Mn}$ and from 2.069 to 2.134 Å for $\text{M}=\text{Ni}$. The shorter M-O distance for $\text{M}=\text{Ni}$ is consistent with it being less polarized and more covalent than for $\text{M}=\text{Mn}$, consequently stronger than that for $\text{M}=\text{Mn}$. The electron density in the interatomic metal oxygen region is growing gradually for $\text{M} = \text{Mn, Fe, Co, Ni}$. For $\text{M}=\text{Zn}$ it is lower than that of Ni, but higher than that of Mn, see ESI, SF4.

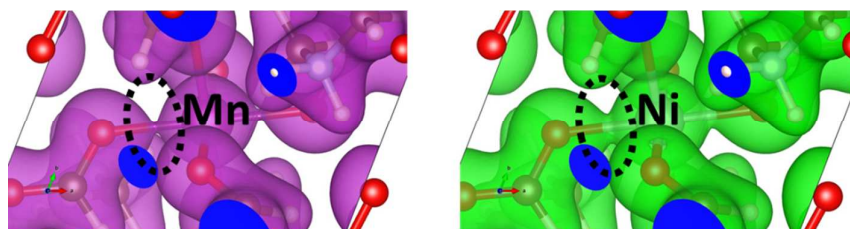


Figure 3. Electron density, at the $0.055a_0^{-3}$ isodensity surface (a_0 : Bohr radius), in $[\text{Me}_2\text{NH}_2] \text{Mn} [\text{HCOO}]_3$, violet, and $[\text{Me}_2\text{NH}_2] \text{Ni} [\text{HCOO}]_3$, green. The metal oxygen interatomic region is encircled with dotted black line. Oxygen atoms are in red. The blue color represents the boundaries of the periodic simulation cell.

Summary and conclusions

In this manuscript, a topological analysis of the electron density of hybrid materials with a perovskite architecture is presented. The Bader-charge partitioning scheme provides valuable physical insight into the variation of the volumes of the metal, dimethylammonium and formate building units. We find that the geometries of the discussed hybrid perovskites depend on the charge transfer between the metal and formate ligands. A greater charge transfer from metal to ligand, $M=Mn$ for example, results in larger cell parameters of the system. As a result of varying metal-oxygen interactions, the size of the dimethylammonium cavity changes as well, although the charge of the organic cation remains practically unchanged. The decreasing polarization of the metal-oxygen bond and the accompanying enhanced interatomic electron density along the discussed transition metal series might account for increasing strength of metal oxygen bond and thus the observed enhanced Young moduli of these systems. The minor variation in Bader charges and volumes as a function of the U parameter makes this method plausible for studying systems containing transition metal oxygen interactions.³⁴⁻³⁶

Acknowledgements

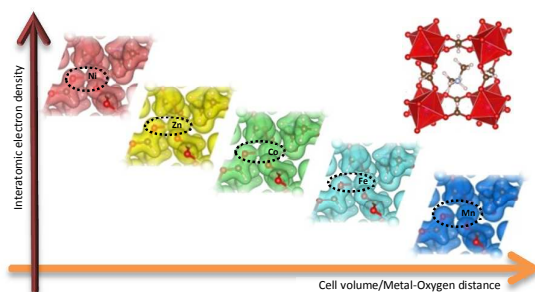
We acknowledge Prof. S. Grimme and Jonas Möllmann for the contribution of the implementation of the DFT-D3 method for the VASP code. MK acknowledges financial support from the Israeli Ministry of Absorption.

References

1. H. Furukawa, K. E. Cordova, M. O'Keeffe and O. M. Yaghi, *Science*, 2013, **341**, 974.
2. *Chemical Society Reviews themed issue on MOFs*
2014.
3. Y. Inokuma, S. Yoshioka, J. Ariyoshi, T. Arai, Y. Hitora, K. Takada, S. Matsunaga, K. Rissanen and M. Fujita, *Nature*, 2013, **495**, 461.
4. A. K. Cheetham, C. N. R. Rao and R. K. Feller, *Chemical Communications*, 2006, 4780.
5. E. Coronado and G. Minguez Espallargas, *Chemical Society Reviews*, 2013, **42**, 1525.
6. C. N. R. Rao, A. K. Cheetham and A. Thirumurugan, *Journal of Physics-Condensed Matter*, 2008, **20**.
7. J. C. Tan and A. K. Cheetham, *Chemical Society Reviews*, 2011, **40**, 1059.
8. X. Y. Wang, L. Gan, S. W. Zhang and S. Gao, *Inorganic Chemistry*, 2004, **43**, 4615.
9. X. Y. Wang, Z. M. Wang and S. Gao, *Chemical Communications*, 2008, 281.
10. P. Jain, N. S. Dalal, B. H. Toby, H. W. Kroto and A. K. Cheetham, *Journal of the American Chemical Society*, 2008, **130**, 10450.
11. P. Jain, V. Ramachandran, R. J. Clark, H. D. Zhou, B. H. Toby, N. S. Dalal, H. W. Kroto and A. K. Cheetham, *Journal of the American Chemical Society*, 2009, **131**, 13625.
12. A. Stroppa, P. Barone, P. Jain, J. M. Perez-Mato and S. Picozzi, *Advanced Materials*, 2013, **25**, 2284.

13. A. Stroppa, P. Jain, P. Barone, M. Marsman, J. M. Perez-Mato, A. K. Cheetham, H. W. Kroto and S. Picozzi, *Angewandte Chemie-International Edition*, 2011, **50**, 5847.
14. D. Di Sante, A. Stroppa, P. Jain and S. Picozzi, *Journal of the American Chemical Society*, 2013, **135**, 18126.
15. J. C. Tan, P. Jain and A. K. Cheetham, *Dalton Transactions*, 2012, **41**, 3949.
16. S. S. Han and W. A. Goddard, *Journal of Physical Chemistry C*, 2007, **111**, 15185.
17. M. Kosa, J. C. Tan, C. A. Merrill, M. Krack, A. K. Cheetham and M. Parrinello, *Chemphyschem*, 2010, **11**, 2332.
18. G. Kresse and J. Hafner, *Physical Review B*, 1994, **49**, 14251.
19. G. Kresse and J. Hafner, *Physical Review B*, 1993, **47**, 558.
20. G. Kresse and J. Furthmuller, *Computational Materials Science*, 1996, **6**, 15.
21. G. Kresse and J. Furthmuller, *Physical Review B*, 1996, **54**, 11169.
22. P. E. Blochl, *Physical Review B*, 1994, **50**, 17953.
23. G. Kresse and D. Joubert, *Physical Review B*, 1999, **59**, 1758.
24. J. P. Perdew, K. Burke and M. Ernzerhof, *Physical Review Letters*, 1996, **77**, 3865.
25. S. L. Dudarev, G. A. Botton, S. Y. Savrasov, C. J. Humphreys and A. P. Sutton, *Physical Review B*, 1998, **57**, 1505.
26. S. Grimme, J. Antony, S. Ehrlich and H. Krieg, *Journal of Chemical Physics*, 2010, **132**.
27. R. F. W. Bader, *Atoms in Molecules: A Quantum Theory; Oxford University Press:Oxford, UK*, 1990.
28. E. Sanville, S. D. Kenny, R. Smith and G. Henkelman, *Journal of Computational Chemistry*, 2007, **28**, 899.
29. G. Henkelman, A. Arnaldsson and H. Jonsson, *Computational Materials Science*, 2006, **36**, 354.
30. W. Tang, E. Sanville and G. Henkelman, *Journal of Physics-Condensed Matter*, 2009, **21**.
31. K. Momma and F. Izumi, *Journal of Applied Crystallography*, 2008, **41**, 653.
32. R. D. Shannon and C. T. Prewitt, *Acta Crystallographica Section B-Structural Crystallography and Crystal Chemistry*, 1969, **B 25**, 925.
33. R. D. Shannon, *Acta Crystallographica Section A*, 1976, **32**, 751.
34. S. H. Wei and A. Zunger, *Physical Review B*, 1988, **37**, 8958.
35. A. J. Cohen, P. Mori-Sanchez and W. T. Yang, *Science*, 2008, **321**, 792.
36. S. Kummel and L. Kronik, *Reviews of Modern Physics*, 2008, **80**, 3.

TOC colour graphic



TOC text:

Charge partition between the metal and the ligand govern the geometry evolution in hybrid perovskites.